

## Air-Sea Transfer of Momentum, Heat and Water Determined from Profile Measurements During BOMEX<sup>1,2</sup>

C. A. PAULSON<sup>3</sup>

*Dept. of Oceanography, Oregon State University, Corvallis 97331*

AND E. LEAVITT AND R. G. FLEAGLE

*Dept. of Atmospheric Sciences, University of Washington, Seattle 98105*

(Manuscript received 7 February 1972, in revised form 8 May 1972)

### ABSTRACT

One hundred forty-one simultaneous wind speed, temperature and humidity profiles measured during the Barbados Oceanographic and Meteorological Experiment (BOMEX) are analyzed. The observations were from heights 2–11 m above MSL and were made from the *R/V Flip*, a research vessel specially designed to be stable at sea. The wind measurements are corrected for the interference of *Flip's* hull with the air flow. Evaporation estimates from the profiles are in fair agreement with simultaneous estimates by the eddy-correlation method. However, the heat fluxes estimated by the two methods are in poor agreement. There appear to be diurnal variations in air temperature, sea surface temperature and stress. The flux of latent heat is large, averaging 17 mW cm<sup>-2</sup>, while the flux of sensible heat is always upward and ~1 mW cm<sup>-2</sup>.

### 1. Introduction

The dynamic and thermal properties of the atmosphere and ocean are directly affected by air-sea transfers of momentum, heat and water vapor. The transfers are nearly independent of height in the atmospheric surface layer, a layer extending from the surface to a height of about 50 m. This enables one to infer the fluxes at the interface from measurements at a convenient height above sea level.

One method of estimating the turbulent fluxes of momentum, heat and water vapor in the atmospheric surface layer is the measurement of the mean vertical profiles of wind speed, temperature and humidity and the use of profile relationships to obtain the fluxes. A set of profile relationships for unstable stratification is obtained by integrating (Paulson, 1970) a flux-gradient relation suggested by Businger (1966) and Dyer and Hicks (1970) to obtain

$$u - u_s = \frac{u_*}{k} \left[ \ln \frac{z}{z_0} - \psi_1(\text{Ri}) \right], \quad (1)$$

$$\theta - \theta_0 = \theta_* \left[ \ln \frac{z}{z_0} - \psi_2(\text{Ri}) \right], \quad (2)$$

<sup>1</sup> Contribution No. 252, Department of Atmospheric Sciences, University of Washington.

<sup>2</sup> Presented at the Conference on the Interaction of the Sea and the Atmosphere, 1–3 December 1971, Ft. Lauderdale, Fla.

<sup>3</sup> Affiliated with the Department of Atmospheric Sciences, University of Washington, during the course of most of the research reported here.

$$q - q_0 = q_* \left[ \ln \frac{z}{z_0} - \psi_2(\text{Ri}) \right], \quad (3)$$

where we define:

$u$	mean wind speed
$u_s$	sea surface drift velocity
$u_*$	friction velocity [ $= (\tau/\rho)^{1/2}$ ]
$\tau$	wind stress
$\rho$	air density, $1.15 \times 10^{-3}$ gm cm <sup>-3</sup> for the observations reported here
$k$	von Kármán's constant (taken as 0.4)
$z$	height above mean sea level
$z_0$	roughness length
$\psi_1, \psi_2$	universal functions of Ri
Ri	Richardson number [ $= (g/T)(\partial\theta_v/\partial z)/(\partial u/\partial z)^2$ ]
$g$	acceleration due to gravity
$T_v$	virtual temperature [ $= T(1+0.61q)$ ]
$T$	mean air temperature
$\theta_v$	virtual potential temperature ( $= T_v + \Gamma z$ )
$\Gamma$	adiabatic lapse rate ( $= g/c_p$ )
$c_p$	specific heat capacity of air at constant pressure
$\theta$	potential temperature ( $= T + \Gamma z$ )
$\theta_0$	value of $\theta$ extrapolated to $z = z_0$
$\theta_*$	scaling temperature [ $= -(1/ku_*)(H/\rho c_p)$ ]
$H$	heat flux density
$q$	specific humidity
$q_0$	value of $q$ extrapolated to $z = z_0$
$q_*$	scaling humidity [ $= -(1/ku_*)(E/\rho L)$ ]
$E$	flux density of latent heat
$L$	latent heat of evaporation

Experimental support for the validity of (1)–(3) has been given by Businger (1966), Dyer (1965), Dyer and Hicks (1970), and Miyake *et al.* (1970). Businger *et al.* (1971) present measurements which differ in some details with (1)–(3), but it seems unlikely that these differences are of significance for the flux computations to be presented here. The use of an identical function of stability,  $\psi_2(Ri)$ , in both (2) and (3) implies that the turbulent transfer coefficients for heat and water vapor are assumed equal. The value of the constant in the  $\psi_1$  and  $\psi_2$  functions is set equal 16 (Paulson, 1970). In the definition of  $Ri$  we have included the effect of the humidity gradient on the density stratification, a factor which is often important over water. Flux estimates are obtained by a least squares fit of  $u$  vs  $\ln z - \psi_1(Ri)$ ,  $\theta$  and  $q$  vs  $\ln z - \psi_2(Ri)$ , giving the slopes  $u_* / k$ ,  $\theta_*$  and  $q_*$  from which  $\tau$ ,  $H$  and  $E$  can be calculated.

The purpose of this paper is to describe an analysis of profile observations made during the Barbados Ocean-

graphic and Meteorological Experiment (BOMEX). The observations are analyzed within the framework outlined above, the resulting flux estimates are compared with other flux measurements, and the temporal behavior of the fluxes is examined.

## 2. The experiment

Observations were made aboard the *R/V Flip* which is operated by the Marine Physical Laboratory of Scripps Institution of Oceanography (Bronson and Glosten, 1968). *Flip* is schematically shown during operating orientation in Fig. 1. The profile mast is located at the end of a boom extending 50 ft from the hull. This mast could be driven horizontally to the end of a catwalk 20 ft from the hull for mounting and servicing instrumentation. *Flip's* orientation with respect to the wind direction (wind blowing into Fig. 1) was maintained by an arrangement consisting of a

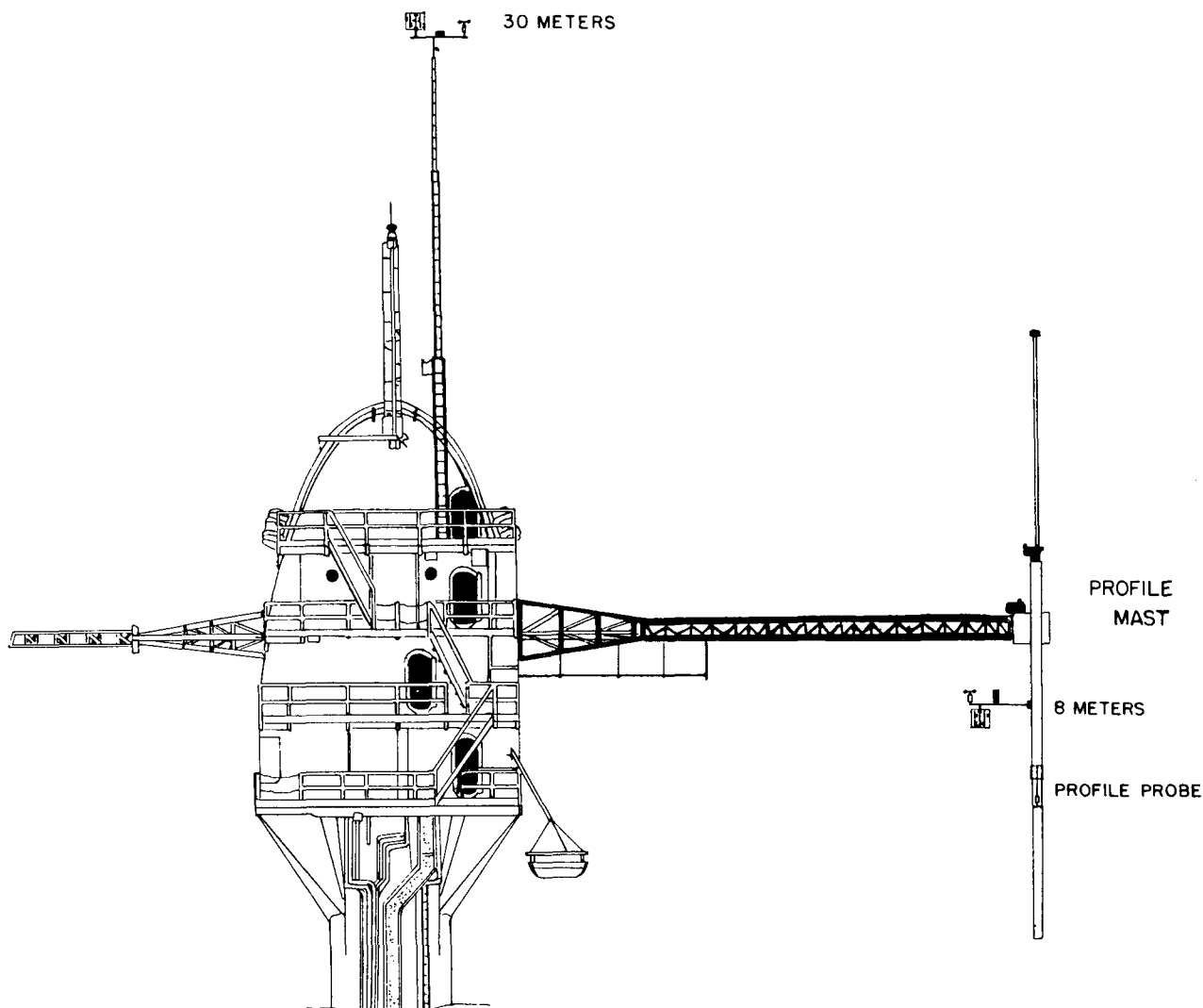


FIG. 1. *R/V Flip* during operating orientation showing the profile mast and the location of turbulence instrumentation at 8 and 30 m.

bridle attached to each side of the superstructure (not visible in Fig. 1) which was in turn attached to a tow-line extending downwind to a tug. Tension on the tow-line caused *Flip* to rotate until the tension in both branches of the bridle was equal. The tug was operated in the direction of the wind vector at 10 rev min<sup>-1</sup> part of the time but even without power the wind force on the tug was usually sufficient to keep *Flip* properly aligned.

*Flip* is very stable compared to an ordinary ship. Vertical displacements were no more than a few centimeters. Pitch and roll motions had angles  $\lesssim 1^\circ$  with a spectral peak characteristic of the wave periods at 6–10 sec. There were also small rotational motions about the vertical axis. All of these motions caused spurious fluctuations of wind velocity measured by sensors mounted on *Flip*. However, they are not expected to seriously affect the averages due to their small amplitude and restricted frequency range.

The profile measurements were made by sampling wind speed, temperature and wet bulb temperature at logarithmically spaced heights, 2 to 11 m above MSL. The probe, shown in Fig. 2, was driven up and down the mast by servo-controlled motor, stopping at four levels for a specified sampling period (usually 20 sec). The probe instrumentation consisted of a Beckman-Whitley cup anemometer and a thermocouple psychrometer. Identical measurements, which were made on a stationary boom at the 8 m level (Fig. 1), were used to correct the profile measurements for sampling error. The details of this correction procedure and a more complete description of a similar system are given by Badgley and Paulson (1972) and Paulson *et al.* (1972). The data were recorded on magnetic tape in analog form and on paper punch tape in digital form for later processing. The length of each run was 48 min, determined by the length of a reel of magnetic tape. The random uncertainties (standard errors) in the profile observations estimated from differences between fitted profiles and observations are: wind speed,

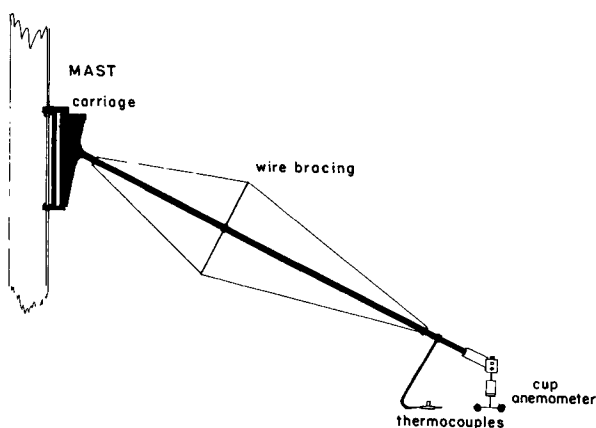


FIG. 2. The profile probe which extends 2 m from the mast and moves vertically on a track.

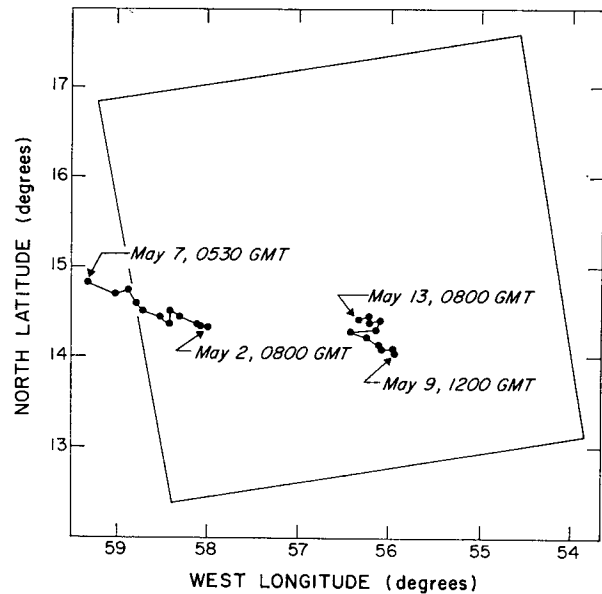


FIG. 3. Recorded positions of *Flip* during the two series of observations. The 500-km square is the BOMEX array.

2 cm sec<sup>-1</sup>; potential temperature, 0.005°C; and humidity, 0.02 gm kg<sup>-1</sup>.

In addition to the profile measurements, various kinds of turbulence measurements at both the 8 and 30 m levels were made by ourselves and by personnel from the University of California at San Diego, the University of British Columbia, and Oregon State University. These measurements included wind velocity components by acoustic anemometers and high-frequency temperature and humidity fluctuations. These measurements permitted computation of the turbulent fluxes by the direct or eddy-correlation method (Pond *et al.*, 1971). Sea temperature was measured by means of a bucket and mercury thermometer. The height of the profile mast above mean sea level was monitored by use of a stilling well consisting of a flexible, weighted length of transparent tubing attached to the mast. A ventilated psychrometer was used to obtain wet and dry bulb temperatures at an upwind deck of *Flip*. Surface drift velocity,  $u_s$ , with respect to *Flip* was estimated by observing the drift of foam floating on the surface. This velocity was always small, typically  $\leq 10$  cm sec<sup>-1</sup>, and was therefore neglected in the analysis.

Observations were made at locations shown in Fig. 3. *Flip* drifted out of the array which necessitated a break in the observations from 7–9 May during relocation. The weather was usually fair with cumulus convection and occasional rain squalls which were more frequent during the last series of observations. Winds were usually steady out of the ENE ranging from 2–8 m sec<sup>-1</sup>. A total of 182 runs were recorded. Of these, 141 were accepted for analysis; the remainder were rejected because of either instrumental malfunction or un-

suitable orientation of *Flip* with respect to the wind direction. The stratification was unstable for all of the runs. The humidity gradient typically contributed about two-thirds to the density gradient. A tabulation of the profiles (uncorrected for structural interference) is given by Paulson *et al.* (1970).

**3. Structural interference**

It was found during the analysis that the measured wind profiles were in error due to the interference of *Flip*'s structure with the flow field. The interference is characterized by: (i) a mean velocity vector pointing about 10° downward from horizontal at the 8 m boom; (ii) the cup anemometer on the boom indicating a mean wind speed about 5% higher than the probe anemometer at the same level; (iii) an anomalous unstable curvature, shown in Fig. 4, of the composite (141 runs averaged together) uncorrected  $u$  vs  $\ln z - \psi_1$  observations which should be linear according to (1); and (iv) anomalously low computed values of drag coefficient for neutral stability at 10 m, averaging  $0.8 \times 10^{-3}$ , compared with the usual value near  $1.3 \times 10^{-3}$ .

Mollo-Christensen (1968) performed a wind tunnel model study to evaluate the effect of *Flip*'s structure on the flow field. He found a horse-shoe-shaped vortex with axis in the horizontal, trailing along the wind down both sides of the superstructure. Looking downwind, the rotation in the vortex is clockwise on the left side of *Flip* and counterclockwise on the right side. He also suggested that the maximum distortion to the wind field would occur in the lowest layers where the gradients of undisturbed mean flow are largest. He found a maxi-

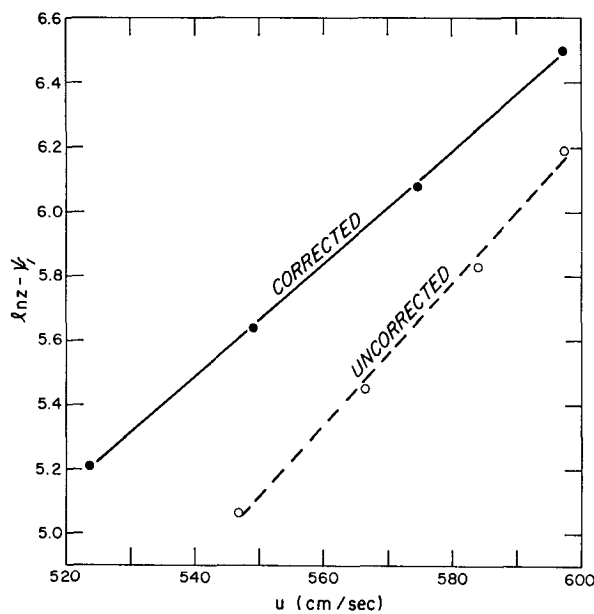


FIG. 4. Composite of 141 wind profiles before and after correction for the effect of structural interference of *Flip* with the air flow.

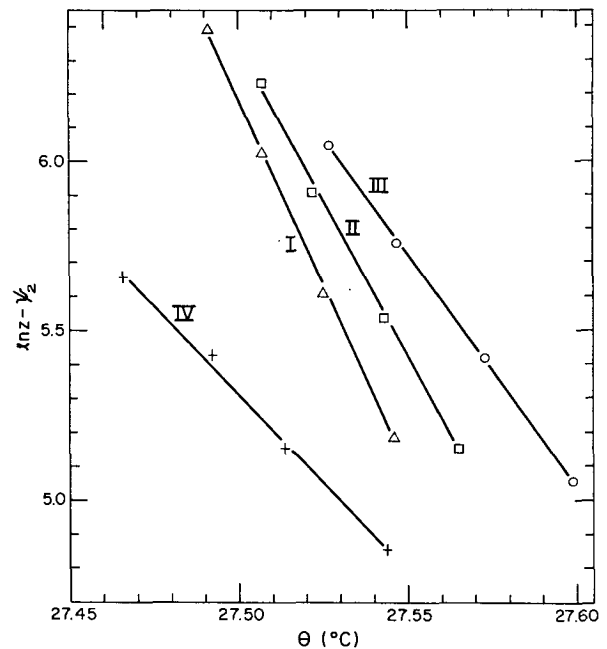


FIG. 5. Composite potential temperature profiles averaged within stability classes given in Table 1.

imum wind speed error of 3% at a scale distance of 37 ft from the model hull.

A qualitative picture of the interference which is consistent with the observed anomalies and the wind tunnel tests shows little effect at the top of the profile, and air descending at middle and lower levels causing an acceleration of the flow and a reduction of the measured wind speed gradient except very near the surface where there would be an increase.

An empirical correction factor was sought which would remove the observed anomalies. The best of several trials is

$$u/u_m = 1 - 0.0021[(\ln z_m)^2 - (\ln z)^2], \quad (4)$$

where  $u$  is the corrected wind speed,  $u_m$  the measured mean wind speed, and  $z_m$  is the maximum measurement height. The constant 0.0021 was chosen so that the stresses computed from the profiles agreed on the average with a limited number of simultaneous direct stress measurements reported by Pond *et al.* (1971). After applying the correction factor to each of the measured wind speeds, one obtains the composite wind profile shown in Fig. 4. The theory fits the corrected measurements better than the uncorrected, and results in a mean drag coefficient for neutral stability at 10 m of  $1.3 \times 10^{-3}$  which is in good agreement with other measurements over the open sea reported by Deacon and Webb (1962), Paulson *et al.* (1972) and Brocks and Krügermeyer (1970). The correction factor leaves the uppermost wind speed unchanged and decreases the lowest measurement by about 5%. The resulting increase in the gradient causes a decrease in the absolute

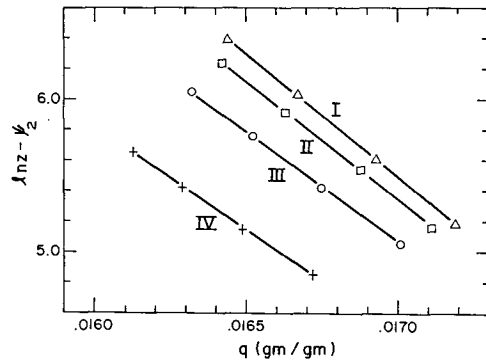


FIG. 6. Composite specific humidity profiles averaged within stability classes given in Table 1.

value of  $Ri$  and a decrease of  $\psi_1(Ri)$  at all heights as shown in Fig. 4.

There is likely some effect of structural interference on the temperature and humidity profiles due to the distortion of mean air trajectories. A downward trajectory increases the magnitude of the temperature or humidity gradient if there is a non-zero gradient in the undisturbed flow. However, no anomalies were observed. The effect of the interference is likely to be less than for wind since distorted trajectories cause the wind to be accelerated in order that mass be conserved, an effect absent for scalar properties.

#### 4. Composite profiles

One may test the accuracy of the temperature and humidity profile relations by plotting  $\theta$  and  $q$  vs  $\ln z - \psi_2$  which ought to be linear according to (2) and (3). We have done this in Figs. 5 and 6 for composite profiles averaged together according to the stability classes given in Table 1. The relations appear to be well satisfied. None of the potential temperature values are more than a few thousandths of a degree Celsius from a straight line and there is little evidence of any systematic deviations. The same holds true for specific humidity where each value is within  $0.02 \text{ gm kg}^{-1}$  of a straight line. These plots attest also to the lack of systematic error in the measurements.

#### 5. Flux comparisons

Runs in which direct flux estimates were made (Pond *et al.*, 1971) and which overlap profile runs are

TABLE 1. Runs grouped according to Richardson number at 5 m above mean sea level.

Group	$Ri$ range	Number of runs
I	$-0.071 < Ri \leq -0.036$	34
II	$-0.093 < Ri \leq -0.071$	36
III	$-0.130 < Ri \leq -0.093$	36
IV	$-1.218 < Ri \leq -0.130$	35

TABLE 2. Runs used for comparison of direct and profile estimates of fluxes during BOMEX. Direct estimates (Pond *et al.*, 1971) are by Oregon State University (OSU) and the University of British Columbia (UBC). Profile estimates (Table 3) are by the University of Washington (UW).

OSU run no.	UW run no.	Overlap (min)
6	20	20
7	21	25
8	44	28
9	47	8
10	59	3
10	60	33
11	76	42
11	77	29
12	94	48
13	127	36
13	128	24
14	132 (40 min)	17
14	133	41
15	147	42
UBC		
run no.		
1	69	40
2	72	45
3	76	42
4	77	28
5	78	44

listed in Table 2. The profile flux estimates for all runs are given in Table 3.

The profile stress estimates are compared with the direct estimates in Fig. 7. Of course, it is no accident that the averages agree since the constant in the wind profile correction formula (4) was chosen to give such agreement. However, it is possible that the wind profile correction might have been improved if the constant 0.0021 in (4) had instead been some function of wind speed and stability. The lack of any systematic variation in the difference between direct and profile estimates as a function of the magnitude of  $\tau$  suggests that any variation of the constant is small. The average magnitude of the difference between profile and direct estimates is 16%, perhaps due partially to the limited overlap of some of the runs.

The heat fluxes are compared in Fig. 8. With the exception of one run, the profile estimates are about one-half as large as the direct estimates. A similar discrepancy between bulk and direct estimates, as well as markedly dissimilar temperature and humidity spectra, were reported by Pond *et al.* (1971). Holland (1972) has suggested that since the potential temperature profile becomes nearly adiabatic due to radiative transfer at about 20 m, heat will be carried upward by buoyant moist eddies more efficiently than would be indicated by the mean temperature gradient. A mechanism suggested by Deardorff (1966), in which turbulent temperature fluctuations are transported upward enabling heat flux in the absence of a mean temperature gradient, may also play a roll. An attempt to modify the profile relation to eliminate the disagreement in heat flux estimates would be premature without

TABLE 3. Stress, heat flux and latent heat flux estimated from profiles during BOMEX.

Date 1969	Run no.	Time begin (GMT)	$\tau$ (dyn cm <sup>-2</sup> )	$H$ (mW cm <sup>-2</sup> )	$E$ (mW cm <sup>-2</sup> )	Date 1969	Run no.	Time begin (GMT)	$\tau$ (dyn cm <sup>-2</sup> )	$H$ (mW cm <sup>-2</sup> )	$E$ (mW cm <sup>-2</sup> )
2 May	1	2210	0.47	0.2	15	7 May	83	0036	0.40	0.9	13
3 May	2	0400	1.27	0.9	20		84	0145	0.30	0.4	9
	3	0513	0.88	0.6	20		85	0355	0.36	0.9	15
	4	0607	0.82	0.6	20		86	0446	0.19	0.7	9
	5	0707	0.66	0.5	16		87	0548	0.12	0.7	8
	6	0800	0.69	0.7	19		88	0700	0.11	0.8	8
	7	0855	0.61	0.6	16		89	0750	0.10	0.8	11
	9	1055	0.58	0.5	16		90	0840	0.16	1.0	13
	10	1152	0.70	0.8	19	9 May	92	1639	1.02	1.8	22
	11	1244	0.60	0.8	18		93	1734	1.11	2.2	27
	12	1337	0.60	0.8	17		94	1908	0.76	2.0	23
	13	1434	0.50	0.9	16		95	1959	0.55	1.4	17
	14	1729	0.30	0.5	12	10 May	96	2053	0.70	1.5	20
	17	2247	0.47	0.6	16		111	1353	0.65	1.2	19
4 May	18	2342	0.44	0.4	17		112	1445	0.47	0.6	18
	19	0330	0.60	0.7	18		115	1834	0.61	1.3	22
	20	0427	0.40	0.7	14		116	1930	0.60	1.6	25
	21	0517	0.69	0.6	18	11 May	120	0018	0.44	0.2	15
	22	0622	0.46	0.7	15		121	0108	0.48	0.4	17
	23	0750	0.51	0.9	15		122	0213	0.56	0.4	17
	24	0845	0.54	0.8	15		123	0320	0.53	0.5	14
	28	1230	0.58	1.1	20		124	0417	0.50	0.6	13
	29	1330	0.51	0.9	16		125	0529	0.56	0.6	16
	30	1529	0.53	0.9	14		126	0623	0.47	0.6	13
	32	1735	0.43	0.7	14		127	0742	0.51	0.6	19
	33	1825	0.54	0.8	17		128	0832	0.64	0.8	22
	34	1921	0.57	1.0	18		129	0924	0.39	0.5	18
	35	2015	0.41	0.4	13		132	1212	0.43	0.5	14
	36	2320	0.71	0.7	18		133	1256	0.46	0.4	15
5 May	38	0123	0.80	0.3	16		135	1515	0.41	0.7	16
	39	0220	1.00	0.3	20		136	1608	0.47	0.7	16
	40	0310	0.94	0.3	19		137	1725	0.72	0.6	18
	41	0405	1.08	0.6	21		138	1816	0.60	0.7	16
	42	0459	0.81	0.7	18		139	1922	0.49	0.4	16
	43	0550	0.85	0.7	20		140	2019	0.61	0.4	18
	44	0642	0.83	0.6	18		141	2125	0.70	0.4	18
	47	1045	0.91	0.6	21		142	2219	0.82	0.3	20
	48	1428	0.70	0.9	18		143	2310	0.74	0.4	19
	50	1754	0.70	0.8	19	12 May	144	0002	0.82	0.5	19
	51	1850	0.69	0.8	18		145	0058	1.07	0.9	24
	52	2000	0.47	0.5	14		146	0150	1.03	0.7	23
	53	2112	0.52	0.4	15		147	0305	0.86	0.8	24
	54	2202	0.62	0.4	13		150	0605	0.46	0.7	17
	55	2255	0.58	0.4	14		151	0705	0.55	0.9	20
	56	2345	0.54	0.4	13		153	0911	0.46	0.8	17
6 May	57	0035	0.76	0.4	14		154	1002	0.30	0.7	14
	58	0138	0.72	0.5	15		155	1053	0.30	0.3	12
	59	0232	0.59	0.5	13		156	1143	0.38	0.2	14
	60	0346	0.62	0.4	13		159	1441	0.34	0.9	14
	61	0440	0.82	0.5	17		161	1959	0.47	0.9	18
	62	0536	0.65	0.6	15		162	2049	0.56	0.9	15
	63	0626	0.62	0.6	14		163	2148	0.56	0.8	20
	64	0720	0.67	0.7	16		164	2242	0.64	0.9	19
	65	0817	0.94	0.9	19		165	2334	0.69	0.8	17
	66	0902	0.85	0.7	17	13 May	166	0026	0.70	0.7	19
	67	0957	1.06	0.9	18		167	0120	1.01	0.7	20
	69	1137	0.87	0.8	21		168	0218	0.85	0.7	23
	70	1237	0.74	0.3	17		169	0330	0.79	0.7	20
	71	1329	0.70	0.6	16		170	0422	0.90	0.9	24
	72	1430	0.53	0.5	14		171	0515	0.76	0.7	21
	73	1520	0.54	0.8	16		172	0608	0.89	0.9	24
	74	1624	0.43	0.6	15		173	0700	0.72	0.9	23
	75	1714	0.46	1.0	16		174	0750	0.57	0.8	17
	76	1810	0.56	0.6	18		175	0843	0.33	0.6	11
	77	1902	0.34	0.4	13		176	0945	0.64	0.5	15
	78	1955	0.26	0.7	13		177	1113	0.73	0.4	17
	79	2046	0.24	0.6	13		178	1205	0.68	0.7	19
	80	2155	0.28	0.7	14		179	1256	0.86	0.7	21
	81	2245	0.36	0.6	13		180	1347	0.89	0.9	23
	82	2345	0.36	1.0	13		181	1442	0.81	0.9	20
							182	1532	0.73	1.4	19

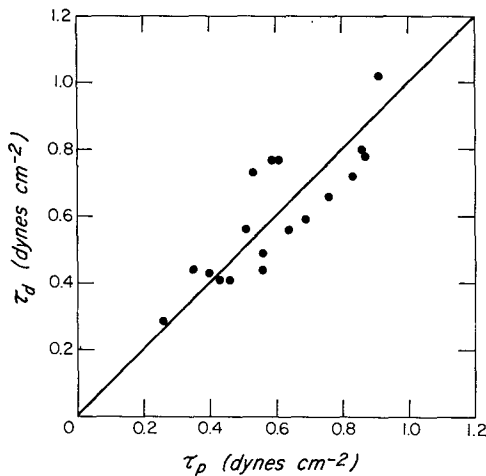


FIG. 7. Direct estimates of stress (Pond *et al.*, 1971) vs profile estimates.

a better quantitative understanding of the mechanisms causing the disagreement.

The evaporation estimates are compared in Fig. 9. The profile estimates are on the average about 25% larger than the direct estimates. Part of this discrepancy may be due to the assumption that the turbulent transfer coefficient for water vapor,  $K_e$ , is equal to that for heat,  $K_h$ . If one had assumed that  $K_e = K_m$ , the coefficient for momentum, the agreement would have been excellent. However, the density stratification is determined primarily by the mean humidity gradient, and buoyancy forces ought to act in the transfer of water vapor as they do for heat. The humidity observations are very well represented by the profile relation with  $K_e = K_h$  as shown in Fig. 6. When  $K_e = K_m$  is used, systematic differences between the observations and the profile relation occur. This suggests that  $K_e$  is nearer  $K_h$  than  $K_m$ . Part of the difference between direct and profile estimates may be due to errors in the direct flux estimates due to limited spectral bandwidth and due to the procedure used to eliminate the effect of structural interference (Pond *et al.*, 1971). The average magnitude of the difference between profile and direct estimates after removal of the systematic difference

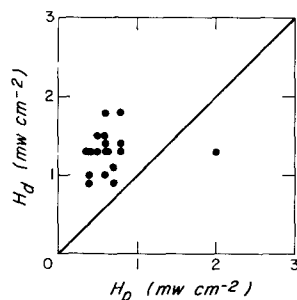


FIG. 8. Direct estimates of heat flux (Pond *et al.*, 1971) vs profile estimates.

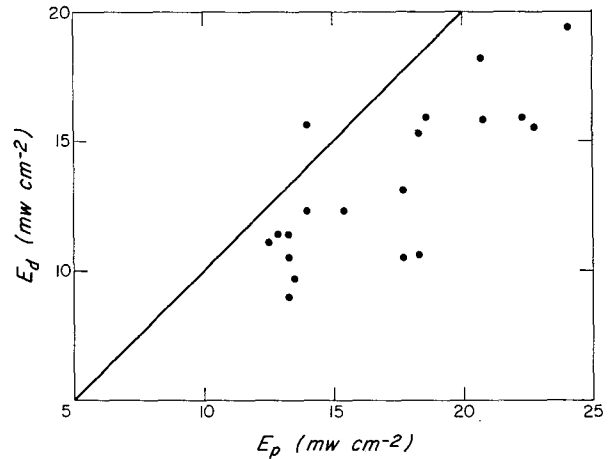


FIG. 9. Direct estimates of latent heat flux (Pond *et al.*, 1971) vs profile estimates.

is 12%. The flux of latent heat averaged over all runs is  $17 \text{ mW cm}^{-2}$  ( $1 \text{ ly min}^{-1} = 69.8 \text{ mW cm}^{-2}$ ) which agrees well with Holland's (1972) summary of  $14\text{--}17 \text{ mW cm}^{-2}$  ( $5\text{--}6 \text{ mm day}^{-1}$ ) for data from various sources in undisturbed periods.

The profile estimates of  $H$  and  $E$  are not very different whether or not the wind profiles are corrected for structural interference. This occurs because of two compensating effects. The wind speed gradient is anomalously small for the uncorrected profiles which results in an anomalously small  $u_*$ . But  $Ri$  is anomalously large because the gradient squared appears in the denominator. This causes  $\psi_2(Ri)$  to be large which gives anomalously large values of  $\theta_*$  and  $q_*$ . The average heat flux for the 19 comparison runs computed from the uncorrected profiles is 10% larger than for the corrected runs, while the average  $E$  is 5% larger for the uncorrected than for the corrected wind profiles.

## 6. Temporal variations

The run averages of  $u$ ,  $T$  and  $q$  at the 11 m profile level and the bucket sea temperature for each run are plotted in Fig. 10. There is evidence of a variation in  $u$  with a period of about 1 day with peaks occurring between 0200 and 0900 GMT. Air temperature shows a diurnal variation due to radiational heating with peaks between 1400 and 2000, minima between 0500 and 0800, and with a maximum amplitude of about 0.5C. Humidity shows evidence of variations of  $\frac{1}{2}$  to  $1\frac{1}{2}$  day period which do not appear to be diurnal. The variations of humidity, and to a lesser extent of temperature, appear to be more erratic and of shorter period during the last half of the observations, probably associated with the greater frequency of squalls during this period. Mean temperature and humidity are both lower during the last half of the observations which indicates greater potential for transfer of sensible and latent heat which is in turn consistent with the observed increase in convective

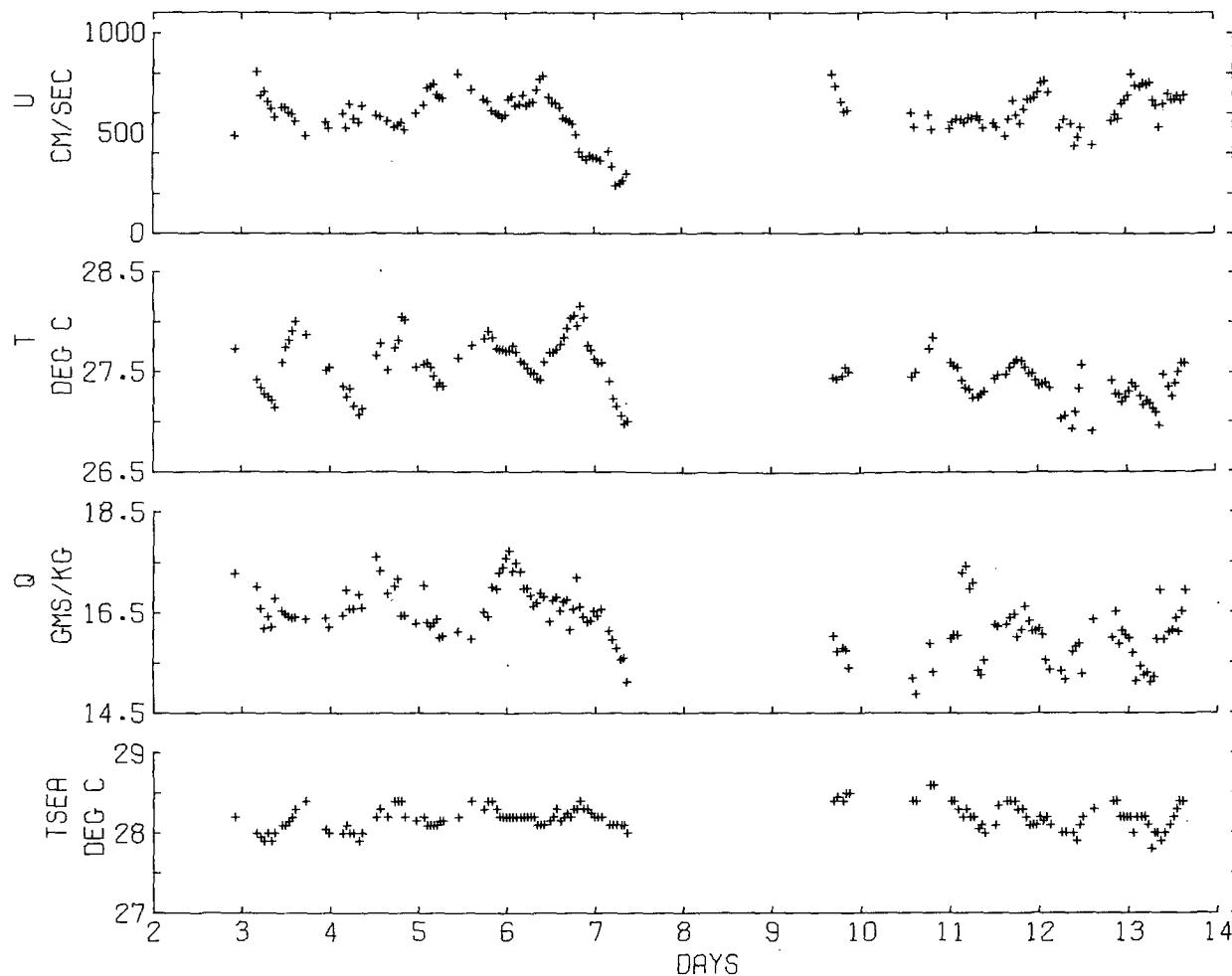


FIG. 10. Average values of wind speed, temperature and humidity from the 11 m profile level and bucket sea temperature as a function of the date (GMT) in May 1969.

activity. Sea temperature has a diurnal variation due to solar heating with maxima between 1600 and 1900 GMT, minima between 0300 and 0900, and with amplitude as large as 0.3C. There are variations in all of the variables from run to run which are probably not entirely due to errors in the observations. For example, on 13 May, the eighth run from the end, there is an anomalously low value of  $u$ , low  $T$  and high  $q$ . There is a log entry for the run indicating that a rain squall was nearby. Other types of disturbances such as secondary flow in the planetary boundary layer (see, e.g., Brown, 1970) may have caused some of the short-period variations. The low values of  $u$ ,  $T$  and  $q$  on 7 May were probably due to synoptic-scale variations.

The observations are averaged in 3-hr intervals according to the time of day in Fig. 11 to show diurnal variations. Trends were not removed. Effects due to the variation of longitude of the observations are ignored because the averaging interval is large compared to the maximum shift (14 min) of local mean time with respect to GMT. The diurnal variations are similar to those

already pointed out, but the amplitudes are considerably less than the maximum amplitudes in the time series due to variations in phase and amplitude. Air temperature has a diurnal amplitude of  $\sim 0.25$ C while the amplitude of sea temperature is  $\sim 0.15$ C. Air and sea temperatures are nearly in phase with maxima and minima near sunrise and sunset, respectively. The sea temperature plot is more regular than the air temperature, probably since air temperature fluctuates more due to turbulence and advection than sea temperature. Wind speed has a peak about midnight local standard time while there appears to be no significant diurnal variation in  $q$ . The good agreement between temperatures and humidities from the profiles and those from the ventilated psychrometer located at an upwind deck give an indication of the accuracy of the measurements, but do not rule out the possibility that the measured diurnal variation of air temperature was exaggerated by errors due to radiative heating of the sensors.

The sea temperature measurements may have been affected by solar heating of the bucket. The samples



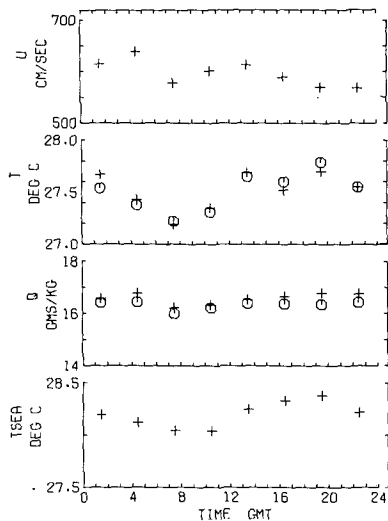


FIG. 11. Crosses indicate 11 m profile values of wind speed, temperature and humidity from a ventilated psychrometer at an upwind deck of *Flip* and bucket sea temperature, all averaged according to the time of day in 3-hr intervals to show diurnal variations. The circles are similar averages for temperature and humidity from the 11 m profile level. Noon (local standard time) is at 1600. The average standard errors for the profile values and sea temperature are:  $u$ , 25 cm sec<sup>-1</sup>;  $T$ , 0.05C;  $q$ , 0.14 gm kg<sup>-1</sup>; and  $T_{SEA}$ , 0.024C.

were taken from the lowest deck of *Flip* with a stained, white plastic bucket. This deck usually faced toward the NE and was shaded by the overhead decks (see Fig. 1). A crude estimate of the change in mean tem-

perature,  $\Delta T$ , of the water sample due to solar heating is given by

$$\Delta T = \frac{Sl^2t}{c_{pw}l^3\rho_w},$$

where  $S$  is the solar constant,  $l$  a typical length dimension of the container,  $t$  the length of time exposed to sunlight,  $c_{pw}$  the specific heat of water at constant pressure, and  $\rho_w$  the water density. A pessimistic estimate of  $\Delta T$  is obtained by substituting  $S=0.14$  W cm<sup>-2</sup>,  $l=25$  cm,  $c_{pw}=4.2$  J gm<sup>-1</sup> (°C)<sup>-1</sup>,  $t=100$  sec, and  $\rho_w=1$  gm cm<sup>-3</sup> which yields  $\Delta T=0.13$ C. This estimate is likely to considerably exceed the actual heating because: 1) part of the radiation striking the bucket was reflected; 2) the bucket was usually exposed to direct sunlight for much less than 100 sec; and 3) when the bucket was exposed for periods as long as 100 sec, the sun angle was low. Typical values of  $\Delta T$  during the day were likely a few hundredths of a degree, probably greatest in the morning because of a favorable sun angle.

A time series plot of the fluxes appears in Fig. 12. The stress appears peaked, having periods from ½–2 days. The heat fluxes are small with periods from a few hours to about a day. There are a few anomalously high values of  $H$  on 9 and 10 May. The evaporation has periods ranging up to about one day with more variability during the second half of the observations with its greater convective activity and higher average evaporation. Some of the peaks in evaporation are associated with the larger peaks in wind stress. Once again there

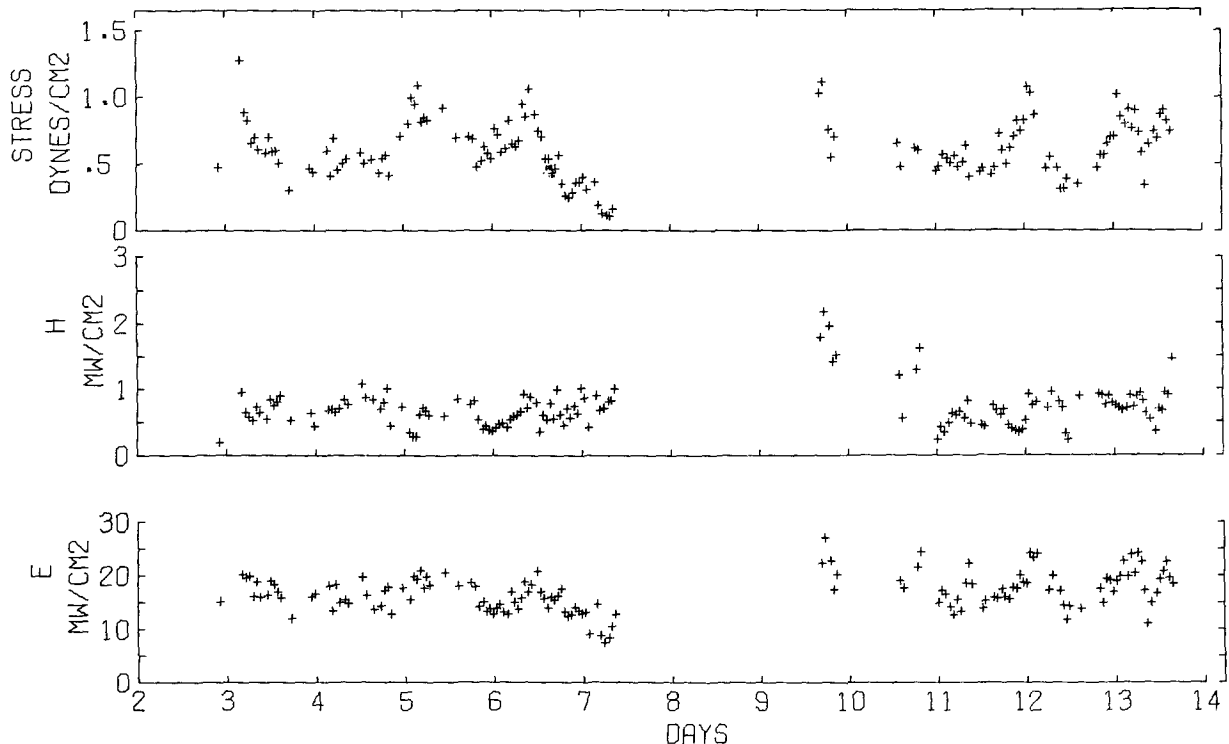


FIG. 12. Profile estimates of stress, heat flux and latent heat flux as a function of the date (GMT) in May 1969.

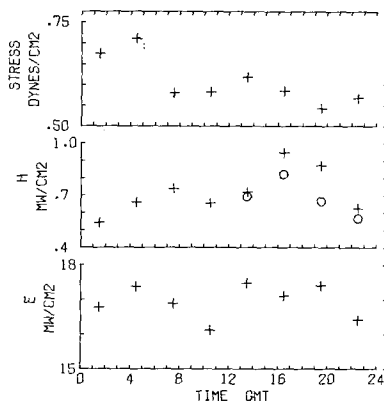


FIG. 13. Profile estimates of stress, heat flux and latent heat flux averaged according to the time of day in 3-hr intervals to show diurnal variations. Noon (local standard time) is at 1600. The circles in the plot of  $H$  are averages neglecting measurements on 9 and 10 May. The average standard error is:  $\tau$ ,  $0.05 \text{ dyn cm}^{-2}$ ;  $H$ ,  $0.06 \text{ mW cm}^{-2}$ ; and  $E$ ,  $0.8 \text{ mW cm}^{-2}$ .

are short period variations in all of the time series due partially to random errors, but perhaps also to mesoscale phenomena.

Diurnal variations of the fluxes are shown in Fig. 13. There is evidence of a diurnal variation in stress with a peak near midnight local standard time, corresponding to the peak in wind speed. The variation of  $H$  is surprising. One would have expected from the behavior of the air and sea temperatures that there would be a diurnal variation of  $H$  with a maximum near sunrise and a minimum near sunset corresponding to maximum and minimum differences in sea and air temperature. There is a small peak near sunrise, but there is another near sunset, even when values from 9 and 10 May are excluded. This anomalous behavior may be due to statistical uncertainty, a variation of the sea surface temperature not reflected in the bucket temperature, errors due to radiation effects on the temperature measurements, or errors in the profile relation which may be a function of solar insolation. There are variations in  $E$  with periods of about 1 day (Fig. 12). However the phase is variable, resulting in no significant diurnal variation in  $E$  (Fig. 13).

## 7. Conclusions

The following conclusions may be drawn:

- 1) There is fair agreement between profile and direct estimates of evaporation. Uncertainties in the profile relation and in the direct estimates may explain the systematic difference of 25%.
- 2) There is poor agreement between profile and direct estimates of the heat flux, the direct values averaging 50% greater than the profile values. The magnitudes of  $H$  are small ( $\sim 1 \text{ mW cm}^{-1}$ ), which may indicate a failure of the profile relation for these small values

(Deardorff, 1966). However, the failure may be peculiarly related to conditions during BOMEX (Holland, 1972).

3) There is evidence of diurnal variations, due to solar radiation, in air temperature and sea surface temperature with peaks in both near 1600 local standard time.

4) There is no evidence of a systematic diurnal variation of evaporation although there are variations of about 1-day period with variable phase.

5) There is evidence of a diurnal variation of stress with a peak near 0000 local standard time. There are variations in stress of 1–2 day period which also appear in evaporation.

*Acknowledgments.* We gratefully acknowledge the effort of the Captain and crew of *Flip* and the staff of the Marine Physical Laboratory in providing for and implementing the use of *Flip* in the experiment. We are grateful to F. Weller and K. Cumle for the development of instrumentation and assistance with the observations. This work was supported by the National Science Foundation under Grants GA-4091 and GA-1099. The later stages of analysis and preparation of the manuscript were also supported by the Office of Naval Research through Contract N00014-67-A-0369-0007 under project NR 083-102.

## REFERENCES

- Badgley, F. I., and C. A. Paulson, 1972: Profiles of wind, temperature and humidity over the Arabian Sea I: The observations. *Intern. Indian Ocean Exped. Meteor. Monogr.*, **6**, 3–29.
- Brocks, K., and L. Krügermeyer, 1970: The hydrodynamic roughness of the sea surface. *Ber. Inst. Radiometeorologie*, **14**, 55 pp.
- Bronson, E. D., and L. R. Glosten, 1968: Floating instrument platform. Tech. Rept., Marine Physical Laboratory, San Diego, Calif.
- Brown, R. A., 1970: A secondary flow model for the planetary boundary layer. *J. Atmos. Sci.*, **27**, 742–757.
- Businger, J. A., 1966: Transfer of momentum and heat in the planetary boundary layer. *Proc. Symp. Arctic Heat Budget and the Atmospheric Circulation*, Santa Monica, Calif., RAND Corp., 305–331.
- , J. C. Wyngaard, Y. Izumi and E. F. Bradley, 1971: Flux-profile relationships in the atmospheric surface layer. *J. Atmos. Sci.*, **28**, 181–189.
- Deacon, E. L., and E. K. Webb, 1962: Interchange of properties between sea and air. *The Sea*, M. N. Hill, Ed., New York, Interscience, 49–87.
- Deardorff, J. W., 1966: The counter-gradient heat flux in the lower atmosphere and in the laboratory. *J. Atmos. Sci.*, **23**, 503–506.
- Dyer, A. J., 1965: The flux-gradient relation for turbulent heat transfer in the lower atmosphere. *Quart. J. Roy. Meteor. Soc.*, **91**, 151–157.
- , and B. B. Hicks, 1970: Flux-gradient relationships in the constant flux layer. *Quart. J. Roy. Meteor. Soc.*, **96**, 715–721.
- Holland, J. Z., 1972: Comparative evaluation of some BOMEX measurements of sea surface evaporation and heat flux. *J. Phys. Oceanogr.*, **2**, 476–486.
- Miyake, M., M. Donelan, F. McBean, C. Paulson, F. Badgley and E. Leavitt, 1970: Comparison of turbulent fluxes deter-

- mined by profile and eddy-correlation techniques. *Quart. J. Roy. Meteor. Soc.*, **96**, 132-137.
- Mollo-Christensen, E., 1968: Wind tunnel test of the superstructure of the *R/V Flip* for assessment of wind field distortion. Rept. 68-2, Fluid Dynamics Lab., M. I. T., 29 pp.
- Paulson, C. A., 1970: The mathematical representation of wind speed and temperature profiles in the unstable atmospheric surface layer. *J. Appl. Meteor.*, **9**, 857-861.
- , E. Leavitt and R. G. Fleagle, 1970: Tabulation of mean profiles of wind speed, temperature and specific humidity for BOMEX, May 2 to 13, 1969. Sci. Rept., Dept. Atmospheric Sciences, University of Washington.
- , M. Miyake and F. I. Badgley, 1972: Profiles of wind, temperature and humidity over the Arabian Sea II: An analysis. *Intern. Indian Ocean Exped., Meteor. Monogr.*, **6**, 33-62.
- Pond, S., G. T. Phelps, J. E. Paquin, G. McBean and R. W. Stewart, 1971: Measurements of the turbulent fluxes of momentum, moisture and sensible heat over the ocean. *J. Atmos. Sci.*, **28**, 901-917.